

PAPER

ANTHROPOLOGY

Carl N. Stephan,¹ Ph.D.

Estimating the Skull-to-Camera Distance from Facial Photographs for Craniofacial Superimposition*†

J Forensic Sci, 2017

doi: 10.1111/1556-4029.13353

Available online at: onlinelibrary.wiley.com

ABSTRACT: The overlay of a skull and a face image for identification purposes requires similar subject-to-camera distances (SCD) to be used at both photographic sessions so that differences in perspective do not compromise the anatomical comparisons. As the facial photograph is the reference standard, it is crucial to determine its SCD first and apply this value to photography of the skull. So far, such a method for estimating the SCD has been elusive (some say impossible), compromising the technical validity of the superimposition procedure. This paper tests the feasibility of using the palpebral fissure length and a well-established photographic algorithm to accurately estimate the SCD from the facial photograph. Recordings at known SCD across a 1–10 m range (repeated under two test conditions) demonstrate that the newly formulated method works: a mean SCD estimation error of 7% that translates into <1% perspective distortion error between estimated and actual conditions.

KEYWORDS: forensic science, craniofacial identification, video superimposition, photography, perspective distortion, subject-to-camera distance

The anatomical comparison of skulls and faces using photographs, otherwise known as craniofacial superimposition, has been a popular tool for excluding individuals in difficult-to-solve cases of questioned skeletal identity (1–6). Sometimes the method has been used as an adjunct to other lines of biological evidence (2), but more controversially (see e.g., (7)), it has also been used as the main line of evidence for identification when other comparative techniques such as DNA or radiographic comparison are not possible (6,8–10).

Since its first derivation in 1934 (11) and application to the forensic context in 1936 (12), the method has found broad use for victim identification across the globe including: USA (5,13), Japan (14), China (15), UK (12), Germany (6), Malaysia (9,16), New Zealand (17), South Africa (18), Chile (7), and Australia (1,19,20). In South Asia and the Pacific, the method has gained unprecedented popularity (9,10,21–23)—on average 58 cases per year were reported between 1970 and 2010 in India, totaling 2307 for this period (9), contrasting with just 14 cases for the FBI across a similar timeframe, 1978–2009 (2).

Despite its less frequent use in the Western world, the method continues to hold value where circumstances limit other options (2,6,13,20,24), and it has featured in some high-profile cases,

such as (i) the *Ruxton Case* or *Jigsaw Murders*, a double homicide from Lancashire, UK, involving the dismemberment of two individuals and the scattering of mutilated body parts around Moffat, Scotland (12); (ii) the identification of the Nazi War Criminal Joseph Mengele in 1985 (25); (iii) Australia's *Truro murders* (20), a seven person serial killing in Adelaide, Australia; and (iv) Australia's largest serial killing case (12 victims), again in the Adelaide district, popularly known as Snowtown's *Bodies-in-the-Barrels Murders* (26,27).

Despite craniofacial superimposition's popularity and contribution toward the successful resolution of some cases, the methods have always been plagued by controversy pertaining to their subjectivity, which has never been effectively removed by the formulation of a strictly scientific approach. Not surprisingly then, highly varied methods (28) have produced highly varied validation test results (18,28–30)—compare, for example, (29) to (18). Charged debates about the methods' utility have consequently ensued (9,18,31), further fuelled by what (until recently) was only one instance in the literature of an erroneous casework conclusion drawn from a flawed superimposition result (32)—a remarkably good track record across a 80-year life span, but one nevertheless potentially skewed by strong publication biases. The recent report of 48 misidentifications from a total of 69 identifications made with heavy reliance on craniofacial superimposition methods from the Patio 29 mass grave (representing secret burials of victims from the 1973 coup in Santiago (7)), raises pressing questions about the superimposition method's reliability and accuracy.

The generic uncertainty associated with superimposition methods has driven some practitioners to err on what is regarded to be safer middle ground: the use of craniofacial superimposition for exclusion only, not for so-called “positive” identifications

¹Laboratory for Human Craniofacial and Skeletal Identification (HuCS-ID Lab), School of Biomedical Sciences, The University of Queensland, Brisbane 4072, Australia.

*Presented in part at the 68th Annual Meeting of the American Academy of Forensic Sciences, February 22–27, 2016, in Las Vegas, NV.

†This study was conducted under The University of Queensland's Behavioural and Social Sciences Ethics Committee Approval #2015001486.

Received 14 Feb. 2016; and in revised form 23 July 2016; accepted 11 Sept. 2016.

(1–7,33,34). However, the aforementioned Snowtown case demonstrates that this is no safety net—a false-negative superimposition result for the first victim left the case unresolved and multiple serial killers at large to commit 11 further murders over multiple intervening years (26,27). False-negative results can thereby be as or more disastrous as false positive identifications. To arrive at an improved craniofacial superimposition approach that carries the highest accuracies possible, a full review and considered analysis of current gaps and weaknesses in the methods is required.

Close inspection of the superimposition method reveals that it is a photographic technique first and an anatomical one-second (1,35). That is, photography of the face results in its point projection as a 3D scene to a 2D plane before any anatomical comparison can be undertaken. The optics of craniofacial superimposition are, therefore, mandatory to master ahead of anatomical comparisons as any optical errors will invalidate the morphological examinations no matter how accurate the latter might otherwise be. The photographic point projection of a 3D scene to a 2D plane generates a distorted view of 3D real-world structure (36,37), which holds major consequences for morphological visualization (1,35,38–40) because the morphology will change between photographs taken at different subject-to-camera distances (35,36,40; Fig. 1), or when subjects are centered differently within the field of view (37,39,41; Fig. 2).

Of the two aforementioned optical parameters, subject-to-camera distance (SCD) and subject position in the field of view, the latter poses little problem as the head position is readily evident in the photograph. Calculating the SCD of the antemortem facial photograph, so that this value can be used to calibrate the skull photography procedure is, however, a much more challenging task. So far, a systematic approach to calculate the SCD from the facial photograph has not only been elusive, but deemed impossible to derive within craniofacial identification circles (30) p. 122–3; (21) p. 118; (23) p. 240. Consequently, present-day options for combating differences in the perspective between the antemortem and postmortem conditions are wholly insufficient and rely on methods that attempt to circumvent determination of the SCD, rather than directly calculating it. These insufficient solutions are briefly outlined below:

- Trial-and-Error Adjustments

Because SCD is deemed impossible to calculate from photographs, trial-and-error approaches have been recommended (21,38). These haphazard attempts, which rely on chance without any systematic protocol, amount to almost pure guesswork. While correct answers may occasionally be generated, it is an inefficient, unreliable, and inaccurate practice.

- Discount the SCD if it is Likely Larger than a Certain Magnitude

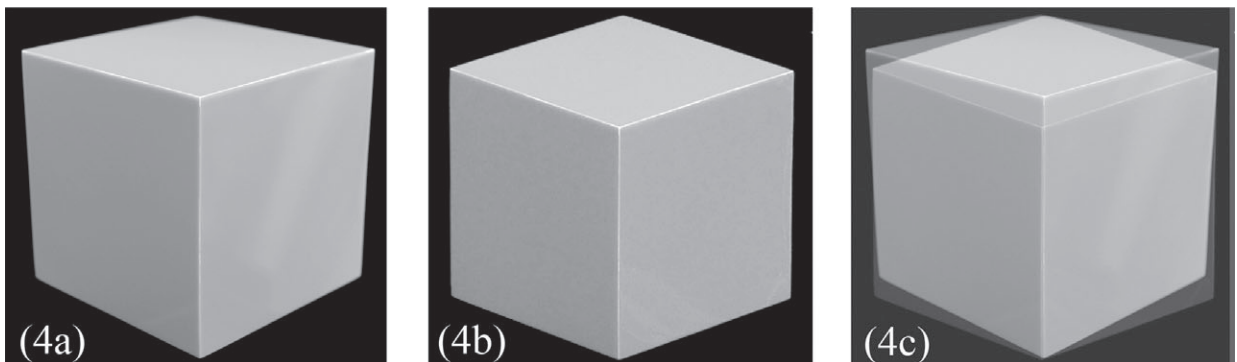
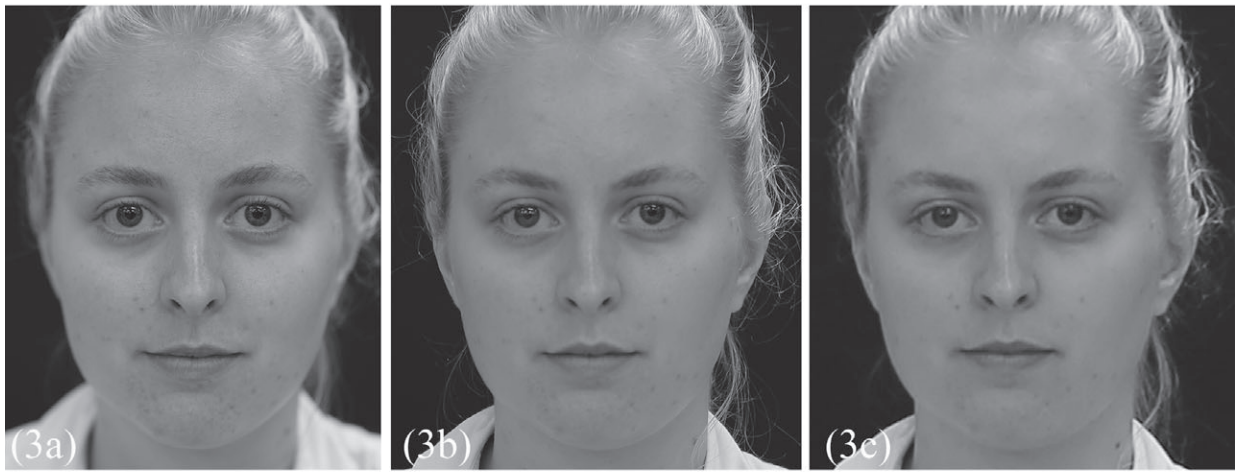
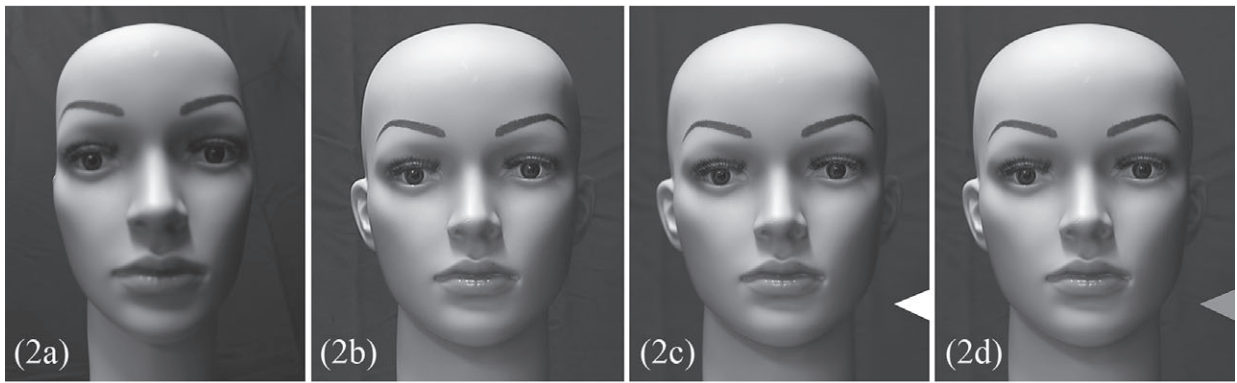
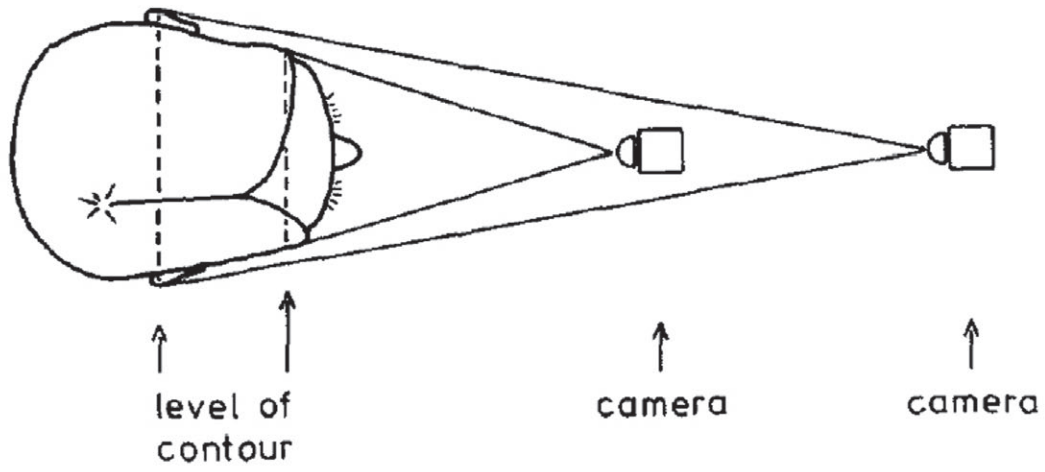
A large proportion of the craniofacial superimposition literature propounds a threshold SCD value at which the perspective distortion is thought to become negligible, so it can be ignored (1,9,12,21,23,30,38,40,42–45; Table 1). This so-called threshold for “no effect” is mistaken. Superimposition requires the comparison of two separately acquired images, one of the face and one of the skull; because each image includes its own perspective, the important factor is not any single measure of perspective, but rather the relative differences in the perspective between the two images (46). This mandates that the SCD always be calculated from the facial photograph and replicated with sufficient accuracy during photography of the skull so that the optics used to view the subjects are near identical (46). It is crucial that the PD in the two photographs is the same, not that one photograph is above or below any threshold. Having one photograph at large distance with so-called negligible PD will be unhelpful if the other image is taken as short SCD with large PD. This complexity is probably the reason for such a large range of threshold values being suggested in the superimposition literature (Table 5) without any consensus on which one should be standard. Further problems with this method arise because SCD cannot currently be estimated in the first place, so practitioners are left to hazard guesses as to whether the SCD used in their particular case is above or below the stipulated threshold.

- Compensate with Zoom

Popular use of dual video cameras to conduct superimpositions offers an enticing capability—tweak the zoom to “help” fit the skull to the face, if SCD is too hard to reliably determine. While the resultant differential image scaling will produce images of similar size for comparison, this approach cannot produce images that are suitable for one-to-one morphological comparison because the perspective between the two is not the same (see Fig. 1). Here we should note that if the camera parameters used to record the facial photograph are replicated for skull photography (i.e., the same format camera is used, the same focal length lens is used, and the same SCD is employed), then the skull and the face will always be at the same raw magnification and at their natural ratio, removing any need for enlargements of either the antemortem face photograph or the postmortem skull photograph.

This point is especially important to emphasize because it has received little attention in the superimposition literature previously, and represents a key change in the superimposition philosophy. In the past enlargement of one or the other images to produce the same relative size has been advocated, see for example, (1). Enlargement of the face photograph to fit the skull (at life size), although seemingly intuitive and broadly recommended (1,9,11,21,22,45–48), unambiguously shows that the antemortem optical parameters have not been precisely replicated

FIG. 1—Different morphologies resulting from different SCDs. Panel 1: Schematic of what the camera sees due to point projection of a face. Image reproduced from Maat (35) p. 232 with permission from Elsevier. Panel 2: (2a) A mannequin head photographed centrally within the field of view of a Canon 6D, fitted with a 24-mm focal length lens, at 0.3 m. Note that the ears are present, but they are hidden behind the cheeks due to the camera's line of sight (refer to Panel 1). Also note major differences in size and proportions of all other facial features compared to (2b). (2b) The exact same mannequin photographed with the same Canon 6D and 24-mm lens, still centrally positioned in the field of view, but at a distance of 1.5 m. Image is rescaled (enlarged) so that face size is the same for both images. (2c) The same mannequin still at a distance of 1.5 m and photographed with the same Canon 6D, but using a 105-mm focal length lens. The image is rescaled for size, but with smaller enlargement than (b). (2d) Superimposition of images (b) and (c) to illustrate that it is not the focal length of the lens that is responsible for perspective distortions—the images precisely superimpose. Panel 3: Face morphology change as a function of SCD: (3a) SCD = 1 m, (3b) SCD = 5 m, and (3c) SCD = 10 m. Photographs have been taken with the same Canon 6D body equipped with a Canon IS f2.8 speed 100-mm fixed macro lens. Face size has been enlarged in (3b) and (3c) at a fixed aspect ratio to match (3a). Panel 4: Morphology change of a cube as a function of SCD to unambiguous illustrates the mismatch. (4a) A 179-mm cube photographed at a distance of 0.7 m. (4b) The same cube photographed with the same camera and lens, but at a camera-to-subject distance of 4.0 m. (4c) Superimposition of (4a) and (4b). Panel 4 reproduced from Stephan (46) p. 257.e4 with permission from Elsevier.



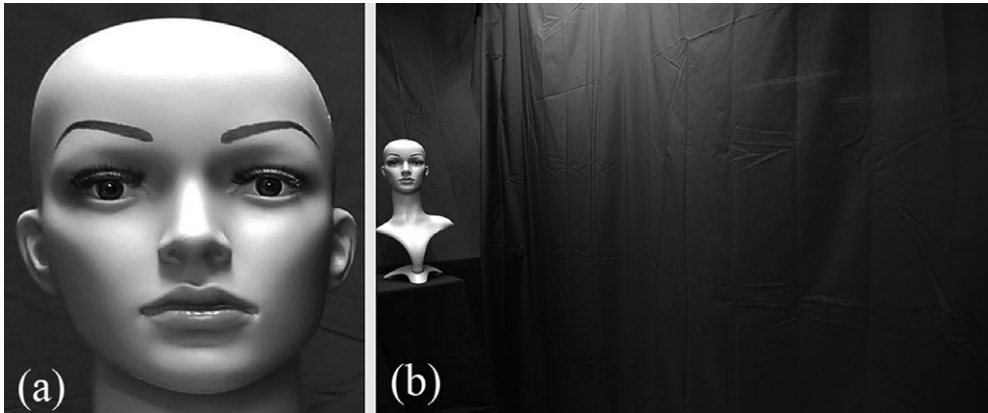


FIG. 2—Perspective distortion due position at the far extreme of the field of view and subsequent stretching across the film plane. (a) Enlarged view of the mannequin head from (b). Note the much broader face and the asymmetry of the face outline compared to Fig 1 where the subject was centrally positioned in the field of view. (b) Full-frame view of the photograph from which (a) was taken.

TABLE 1—Previously reported subject-to-camera distances (floor values) at which perspective distortion is thought to be negligible. Reprinted from Stephan (46) p. 257.e2 with permission from Elsevier.

Subject-to-camera distance (m)	References
1	Sekharan (23) Lan and Cai (30)
1.5	Jayaprakash et al. (16) Glaister and Brash (12) Grüner and Reinhard (42)
2	Miyasaka et al. (43)
2.5	Eliášová and Krsek (44)
3	Titlbach (40)
5	Scully and Nambiar (38) Hashimoto (45)

for the skull photography—otherwise the enlargement would not be required—and this risks error. Contrary to popular thought, life-size enlargement of the facial photograph is not a requirement for superimposition. Rather, the antemortem face image should serve as the overarching and supreme reference standard as it is the identity decider, and the entire superimposition procedure should be orientated toward replicating the antemortem photographic conditions. As stated above, if the skull photography condition matches precisely the antemortem conditions used for face photography, then the two subjects (the face and the skull) will be at their natural ratios, removing any need for differential enlargement of any image relative to the other one. This applies whether the skull is being viewed live through a camera lens, videotaped, or recorded as a still photographic image.

Enlargement problems, of course, do not apply to dual scaling of the face and skull images using the exact same enlargement parameters, as sometimes useful to facilitate enlarged views that enable detailed morphological examinations; but it is important to note here that when low-resolution raster format images are encountered enlargement decreases the overall image quality reducing the utility of this undertaking.

- Use the Metadata

Recent recommendations from the European Commission’s New Methodologies and Protocols of Forensic Identification by Craniofacial Superimposition (MEPROCS) direct practitioners to extract the SCD from the metadata if the antemortem facial photograph is an electronic one (28). While metadata are a reliable

and useful record for some camera parameters (see below), SCD does not currently belong to this class because *focus distance* is not a standard report and when it is recorded, it is often a bracketed range, not a point estimate. Consequently, practitioners risk considerable error if relying on bracketed distances from the camera metadata for estimating the SCD.

- Ask the Photographer Who Took the Original Facial Photograph “What SCD was Used?”

This is perhaps the best of all the above options, but it can only be used infrequently and in limited circumstances as the photographer is not always known or traceable (1). Even if the photographer is located, the method risks recall inaccuracies.

A New, Improved, and Direct Technique to Estimate Subject-to-Camera Distance from Frontal Face Photographs

Ideally, SCD should be estimated directly from the facial photograph and the method used should meet two prerequisites:

- It should be applicable to a broad range of facial photographs, especially those where the person is looking directly at the camera. It must also be usable on facial photographs that do not include extraneous inanimate objects and, therefore, must rely solely upon the facial morphology.
- It must be accurate—a method producing only several millimeters of perspective distortion at life-size will be fatal for precise anatomical comparisons at subsequent steps. Therefore, a workable tolerance range of $\leq 1\%$ perspective error is reasonable. For physiognomical facial height, the error then would correspond to $\leq 1.7\text{--}1.8\text{ mm}$ based on anthropometric data for adults after Farkas et al. (47).

Recently, the perspective distortion (PD) associated with a particular SCD has been mapped for a plexiglass cube constructed with cord lengths approximating craniofacial dimensions (46). This shows that a (within photograph) PD value of 1% is attained at a SCD of 12 m; and in a relative sense between two images there is a range of SCD in which 1% relative PD will not be exceeded. The logarithmic relationship of the PD to SCD mandates a higher SCD precision for short face-to-camera distances than longer ones (46). This works in favor of craniofacial superimposition as photography at short distances provides higher resolutions of subjects that facilitate these higher measurement precisions. If a 1% tolerance for PD mismatch is

accepted, then the SCD for skull photography would need to replicate the face photograph within c. 0.1 m at a SCD of 1.0 m, or alternatively, within a 5.9 m SCD error window at 12.0 m (46).

To calculate the SCD from a facial photograph then, all that is required is an anatomical trait that is relatively invariant between individuals of a given age and sex so that a mean parameter or sample value can be substituted for the individual's true (but unknown) value. In addition, a well-established and basic photographic formula after Kingslake (37) is required:

$$\text{SCD} = f(1 + A/(x * y)) \quad (1)$$

where:

SCD, subject-to-camera distance (mm); f , focal length of the lens (mm); A , real-life object size (mm); x , object size measured on the photograph (pixel units); y , manufacturer's specifications of image receptor pixel size (mm).

In terms of the anatomical trait to be used as the referent, the palpebral fissure length stands out as a prime candidate because it:

- Is easily viewable on anterior view photographs, and it is easily determinable on the side closest to the camera if the head is rotated;
- Is defined by two readily determinable Bookstein (48) type I landmarks (endocanthion and exocanthion), which are regarded to be the most accurate type of landmark class (48);
- Possesses a very tight variation range constrained by evolutionary constraints on the visual system (SD = 1.2 mm for adult males and females), so that the mean value can be used as a good proxy for all individuals of that age and sex, even when the exact palpebral fissure length of the subject is unknown;
- Is a relatively large facial feature (mean = 31 mm; range = 27–35 mm (49)), so the impact of any measurement error is minimized—compare to other invariant traits such as the iris diameter: mean = 12 mm; range = 10–13 mm (50));
- Is a normally distributed character so that the maximum residuals between the real and proxy (mean) value can never exceed half of the distribution range. This effectively cuts the prediction error in half, which is especially useful where true palpebral fissure lengths for particular individual cannot be determined (such as when skeletons of descendent are employed). The variance can also be used to estimate the 99% confidence limit of the SCD estimation, as preferable to a stand-alone and single point estimate.

Items 3, 4, and 5 work together to minimize the residual error (between the mean and ground truth value) providing a good chance that any resulting inaccuracy of a mean does not cause the perspective between the AM and PM photographs to exceed 1%. This can be modelled theoretically using the worst case scenario where the mean palpebral fissure length is a poor proxy to an individual's true value. Take, for example, an extreme male adult who falls at the far right tail (99% confidence limit) of the palpebral fissure length distribution using anthropometrics provided by Farkas et al. (47): 31.3 mm (mean) + [1.2 mm (SD) * 2.575]. In this instance, the palpebral fissure point estimate (31.3 mm) would be a 3.09 mm underestimate of the true value possessed by the subject (34.39 mm). Consequently, equation (1) can be rearranged to solve for the size of the palpebral fissure on the sensor (mm), for example, when a 100-mm lens (f) is used in conjunction with the (poorly applicable) mean palpebral fissure

length of 31.3 mm (A). The result can then be re-substituted back into the same equation at different SCD (1–10 m) along with the ground truth palpebral fissure measurement (34.39 mm) to estimate the (known) SCD, which now gives the error component associated with the mean variable (Table 2). Compared to Stephan's Fig. 3 (46) or Table 3 provided herein, it is clearly apparent that the resulting change of perspective between the estimated and ground truth distances cannot exceed 1%.

The other two variables required for the SCD equation—the camera type (to obtain manufacturer's specifications of image receptor pixel size) and focal length of the lens—can always be reliably extracted from electronic images using free Exif readers available on the Internet (see Materials and Methods for details). As it is best practice to always use an antemortem photograph that has been taken close to the time of an individual's death, availability of metadata for facial photographs will become more common in the future as wet film technology becomes further obsolete and replaced by digital equipment. Of course, the methods described above can still be employed for traditional wet film if the focal length of the lens used is known by tracking down the photographer who took the image, and by replacing the $x*y$ component of Equation (1) with the palpebral fissure distance measured directly on the film negative or from the full-frame image print after adjustment for enlargement from the raw native film format (palpebral fissure length measurement on the print (mm) * [the width of the negative (mm)/width of the print image (mm)]).

Consequently, the above-described new method is best executed in a simple five-step process as follows:

1. Acquire the camera brand, camera model, and focal length size from the image metadata (or seek the photographer who took the original image if analyzing traditional wet film);
2. Obtain the pixel specifications for the digital camera model used (e.g., from the manufacturer's website; ignore this step if analyzing wet film);
3. Extract mean palpebral fissure length from the scientific literature corresponding to the subject in question (e.g., match sex and ancestry as closely as possible), for example, using the anthropometric data reported by Farkas et al. (47).
4. Measure the palpebral fissure length on the photograph in pixel units (or if using wet film, measure the distance directly on the negative or undertake a conversion from the full-frame image print as described above);
5. Use the above-described photographic formula to calculate the SCD.

TABLE 2—Error component using Farkas et al. (47) sample mean data for Caucasoid males aged 19–25 years as a proxy for an individual value that falls three z-scores into the right tail of the distribution.

Ground Truth SCD	Size of Palpebral Fissure Length on the Image Receptor ($x*y$) for the Mean Proxy (31.3 mm)	SCD using proxy on film, but real Palpebral Fissure Length for A (34.39 mm)	Estimated SCD in meter units (m)	Error (m)
1	3.478	1089	1.09	0.09
2	1.647	2188	2.19	0.19
3	1.079	3286	3.29	0.29
4	0.803	4385	4.39	0.39
5	0.639	5484	5.48	0.48
6	0.531	6582	6.58	0.58
7	0.454	7681	7.68	0.68
8	0.396	8780	8.78	0.78
9	0.352	9879	9.88	0.88
10	0.316	10,977	10.98	0.98

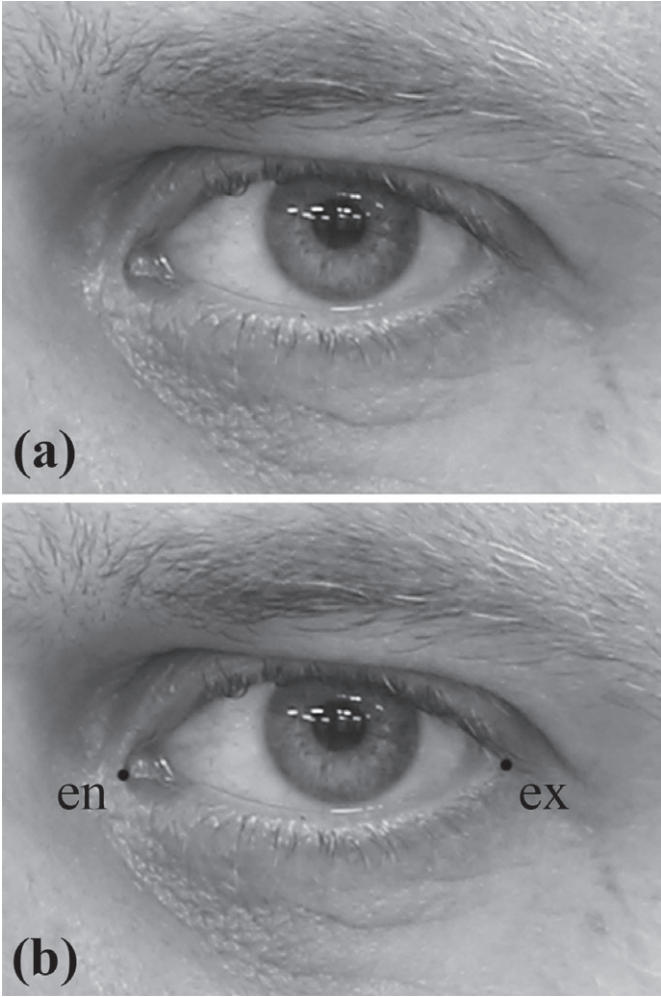


FIG. 3—Positioning of endocanthion and exocanthion landmarks on frontal face photographs. Here placement for a 38.5-year-old subject is illustrated without annotations (a) and with annotated landmarks (b) for the left eye at SCD = 2 m using Canon 6D full-frame 20.2-megapixel camera body fitted with a Canon IS 2.8 speed 100-mm fixed macro lens.

For convenience, this method will hereon be referred to as *PerspectiveX*.

There are two assumptions of the *PerspectiveX* method. First, it assumes the facial photograph has not been cropped (e.g., edges of the image removed giving the impression of different field of view). This can, in part, be cross-checked by referencing the image dimensions in pixels to the sensor specifications provided by the manufacturer for the camera make and model. Second, it assumes a full-frame (35 mm equivalent) image sensor has been used to acquire the image, removing the need for scaling factors to be applied. If a 35-mm format camera has not been used, then additional calculations can be employed to enable *PerspectiveX* to be undertaken, but in the interests of maintaining simplicity for this paper, only the full-frame 35-mm digital SLR camera condition will be considered.

The aim of this study was, therefore, fourfold: (i) to test the performance of the *PerspectiveX* algorithm using facial photographs of known SCD; (ii) to compare these SCD accuracies to those obtained from *focus distance* reports from the camera’s metadata; (iii) to explore the fidelity of the *PerspectiveX* method for facial photographs where the subject’s head is not looking directly toward the camera; and (iv) explore the repeatability and robustness of the method across several subjects (including adults and subadults) and environments (different lighting and camera operators).

Materials and Methods

Study 1: Validation Tests of the *PerspectiveX* method and Comparison to Metadata “Focus Distance”

Four subjects (two adults and two children; Table 4) were photographed at known distances—every whole meter integer between 1 and 10 m—using the same Canon 6D full-frame 20.2-megapixel camera body (image sensor size = 35.8 × 23.9 mm; pixel size = 6.55 μm [square]) fitted with the same Canon IS 2.8 speed 100-mm fixed macro lens. Subjects were seated at the time of photography and asked to look directly at the camera (Fig. 4). Subject 3 was photographed by a different camera operator.

The camera was first centered at the 10 m mark, and then moved to the 1 m mark to initiate the photography sequence so that the face was always centered in the field of view without requiring physical adjustment (camera tripod was simply positioned at the corresponding distance mark). The camera body was supported on a Vanguard Alta Pro Series 70 tripod with plumb line attached to the hook on the central column for accurate placement at one-meter-distance marks indicated on the floor by a spool tape. A Vanguard PH Series Pan Head attached the camera to the tripod. At each new distance, the *camera tripod* was orientated to point at the subject, auto-focus engaged, and the camera shutter released without any manipulation of the camera or the pan head device. No flash units were used to illuminate the subject. Only ambient room light from ceiling-mounted fluorescent globes was used as the light source.

Resultant uncropped images (5472 × 3648 pixels) were imported to Adobe Photoshop CS6 where the left palpebral fissure was measured with the measurement tool in pixel units (Fig. 4). In this study, the exocanthion was placed, not on the scleral junction with the eyelid, but on the external edge of the palpebral fissure (Fig. 3). Equation (1) was then employed to calculate the SCD using the following parameters: $f = 98.7$ (mm; 35 mm equivalent of the 100-mm lens used as read off the

TABLE 3—Upper and lower bounds for SCD mismatch using a PD threshold of ±1% for a 179 mm linear distance (a proxy to adult physiognomical face height), modelled after Stephan (46).

SCD (m)	SCD Mismatch (±1% PD at a 0.1-m resolution)	
	Lower Bound (m)	Upper Bound (m)
1	0.9	1.1
2	1.7	2.4
3	2.4	4.1
4	3.0	5.8
5	3.5	8.1
6	4.0	10.9
7	4.4	14.8
8	4.8	19.4
9	5.2	>20.0
10	5.7	>20.0
11	6.0	>20.0
12	6.2	>20.0
13	6.3	>20.0
14	6.7	>20.0
15	7.1	>20.0

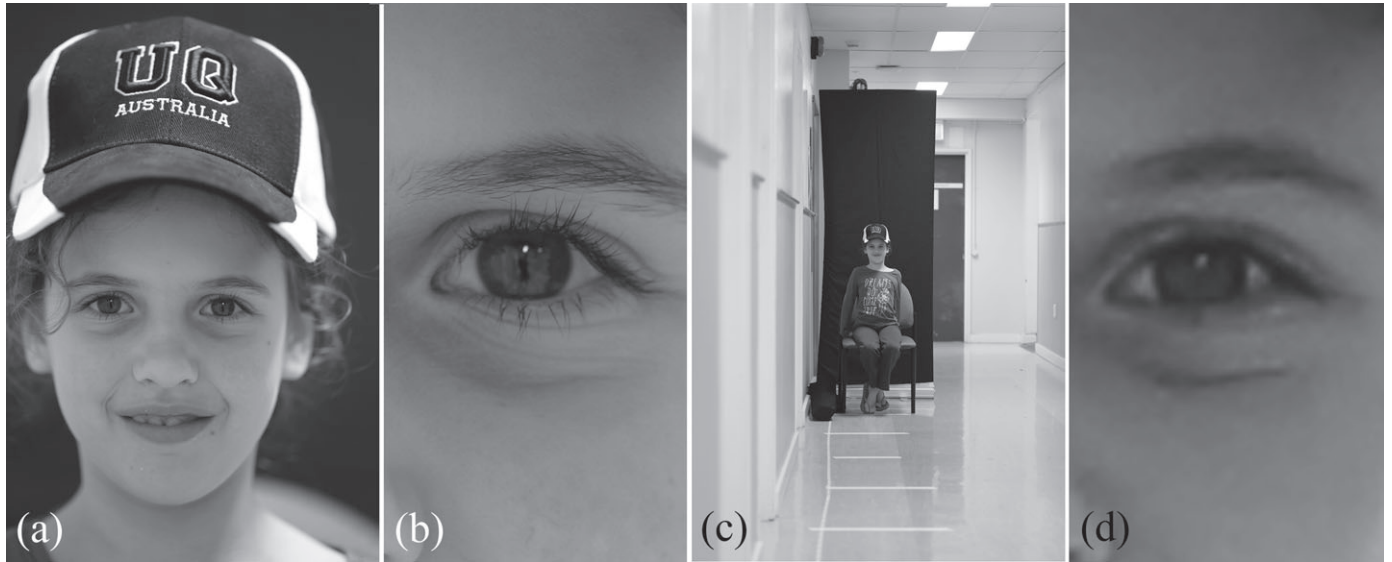


FIG. 4—Examples of eye morphology and photographic quality resulting from the different SCD distances for the 9-year-old participant in Study 1. (a) SCD = 1 m. (b) close-up of left eye in (a) as undertaken for measurement in Adobe® Photoshop®. (c) SCD = 10 m. (d) close-up of left eye in (c) as used for measurement in Adobe® Photoshop®. Note the accuracy for this subject is still high (Table 5) despite long eyelashes obscuring the exocanthion landmark.

TABLE 4—Age (yrs) and sex of participants in this investigation.

	Subjects			
	1 Female	2 Female	3 Male	4 Male
Study 1 Sample (Anterior Face View Only)	44	9	38	7.5
Study 2 Sample (Anterior and Rotated Faces)	22	25.5	20*	38.5

*This subject was of Asian extraction, and so, the 18-year-old Chinese palpebral fissure length datum from Farkas et al. (51) was used for this subject. All other subjects were Caucasoids, and so, palpebral fissure lengths for Caucasoids after Farkas et al. (49) were used for these subjects.

Canon 6D image metadata); A = mean palpebral fissure lengths for American Caucasoids after Farkas (49)—varies by age and sex for each participant; and $y = 0.00655$ (mm).

As each subject was wearing the same baseball cap at the time of photography, the cap insigna could additionally be used to calibrate the palpebral fissure length measurements according to their life-size values and measure any resultant drop in accuracy using the biological referent alone without insigna calibration. The distance that the letters “AUSTRALIA” spanned on the front of the cap was used wherever possible (real-life width = 57 mm) because this insigna fell close to the focal plane of the face, was orientated mostly perpendicular to the lens without too much oblique inclination, and was unlikely to have its position inadvertently adjusted by the subject between photographs. Where the use of this insigna proved challenging due to cap orientation (subject 4), the span across the “UQ” (60 mm) or the distance between the white stripes on the cap peak (114 mm) was instead used (see Fig. 4).

Camera metadata (see e.g., Fig. 5) were used to estimate SCD and gauge its reliability both within and between several cameras that were investigated for this part of the study. The aforementioned full-frame Canon 6D, used for the *PerspectiveX* tests, was included and was further supplemented by data from a full-frame Nikon D700 and five point-and-shoot-style cameras (Olympus

Stylus 790SW, Olympus SP510UZ, Olympus 590UZ and Sony Cybershot G) that separately recorded a single object at the same meter interval spacing used above for the *PerspectiveX* validation. Image metadata were examined using the freely available *ExifTool* (v9.98) by Phil Harvey (www.sno.phy.queensu.ca/~phil/exiftool/) and *Jeffrey's Online Exif Viewer* (<http://regex.info/exif.cgi>). As *Jeffrey's Online Exif Viewer* provided the same values as the *ExifTool*, but to two decimal places less, only results from the *ExifTool* are reported here.

Study 2: *PerspectiveX* Fidelity for Laterally Rotated Faces and Repeat Validation

To cross-check the fidelity of the *PerspectiveX* method for rotated faces and under different environmental conditions, the *PerspectiveX* component of study 1 was repeated but with the following three modifications: (i) subjects' heads were photographed in four degrees of head rotation (c. 0, 10, 20, and 30 degrees; Fig. 6); (ii) three individuals were exchanged for new participants, thereby all subjects in study 2 were adults and one of the new subjects (#3) was of self-reported Asian extraction, and so, the palpebral fissure length for 18-year-old Chinese Males after Farkas et al. (51) was used as a proxy for this individual instead of the Caucasoid data (Table 4); and (iii) the photography location was changed from a fluorescent lit corridor to a fluorescent lit room. The range of head rotations from 0 to 30° is a considerable amount, enough to make the lateral canthus for the eye furthest from the camera invisible on the photograph in the 30° rotation condition, thus representing an extreme three-quarter view (Fig. 6). Subject 4 was photographed by a third camera operator, who did not participate in study one.

Results

SCD Estimation Using *PerspectiveX*

PerspectiveX provided a grand error of 6.6% in estimating SCD with a standard deviation of 2.2%, ranging from a mean of

```

Canon Flash Mode          : Off
Continuous Drive         : Single
Focus Mode               : One-shot AF
Record Mode              : CR2+JPEG
Canon Image Size         : Large
Easy Mode                : Scene Intelligent Auto
Digital Zoom             : None
Contrast                 : Normal
Saturation               : Normal
Camera ISO               : Auto
Metering Mode            : Evaluative
Focus Range              : Not Known
Canon Exposure Mode      : Easy
Lens Type                : Canon EF 100mm f/2.8L Macro IS USM
Max Focal Length         : 100 mm
Min Focal Length         : 100 mm

//

Live View Shooting       : On
Focus Distance Upper     : 20.47 m
Focus Distance Lower     : 6.34 m
Flash Exposure Lock      : Off
Internal Serial Number   : GD1064047

//

Aperture                 : 2.8
Drive Mode               : Single-frame Shooting
File Number              : 100-1977
Image Size               : 3648x5472
Lens                    : 100.0 mm
Lens ID                  : Canon EF 100mm f/2.8L Macro IS USM
Megapixels              : 20.0
Scale Factor To 35 mm Equivalent: 1.0
Shooting Mode            : Scene Intelligent Auto
Shutter Speed            : 1/80
Create Date              : 2015:07:22 18:12:57.87
Date/Time Original       : 2015:07:22 18:12:57.87
Modify Date              : 2015:07:22 22:17:11.87
Thumbnail Image          : <Binary data 3939 bytes, use -b option to extr
act>
WB RRGB Levels           : 1893 1024 1024 2180
Blue Balance             : 2.128906
Circle Of Confusion      : 0.030 mm
Depth Of Field           : 3.08 m <12.04 - 15.12 m>
Field Of View            : 20.7 deg
Focal Length             : 100.0 mm <35 mm equivalent: 98.7 mm>
Hyperfocal Distance      : 117.37 m
Lens                    : 100.0 mm <35 mm equivalent: 98.7 mm>
Light Value              : 5.6
Red Balance              : 1.848633
-- press any key --

```

FIG. 5—Example of abridged metadata record of the Canon 6D, as accessed using ExifTool, for the female adult subject photographed at the 5 m position in Study 1. Note the Lens Type specification in the upper panel; the Focus Distance Upper and Lower in the middle panel; and the Focal Length in the lower panel. Also note that SCD for this image was 5 m, yet the Focus Distance Upper reads 20.47 m and the Focus Distance Lower reads 6.34 m.

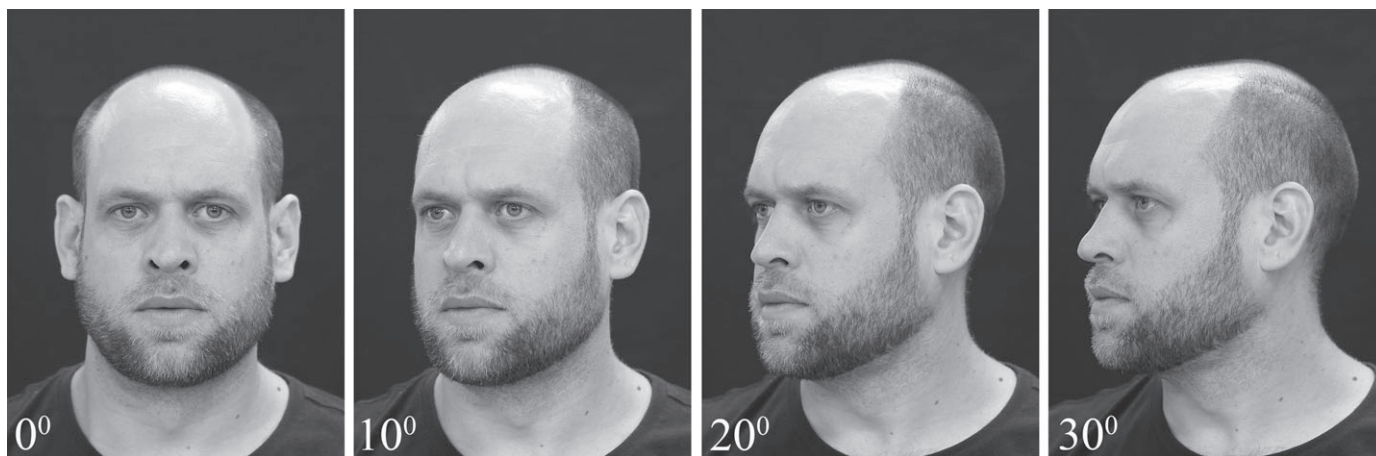


FIG. 6—Examples of the 0, 10, 20, and 30 degrees of head rotation used in Study 2. Images have been cropped to show just the face and were acquired with the Canon 6D full-frame 20.2-megapixel camera body fitted with a Canon IS 2.8 speed 100 mm fixed macro lens at a SCD of 3 m.

2.2% (1 m) to 9.1% (5 m) (Table 5). To put this in context, a 6.6% error at 1 m SCD is less than 7 cm. At 10 m, the error is just below 0.5 m. The PD difference resulting between the ground truth and the estimated SCD, for the same subject, at

physiognomical face height was well below 1% for all these measurements (Tables 3 and 5). This validates the use of the mean palpebral fissure length to estimate SCD in craniofacial superimposition when the focal length of the lens used to take

TABLE 5—Mean SCD estimation in Study 1 using *PerspectiveX* for two adults and two subadults.

Ground Truth SCD (m)	<i>PerspectiveX</i> Estimated SCD (m)					Mean Error (m)	Mean Error (%)
	Subjects				Mean		
	1	2	3	4	Mean		
1	0.95	1.04	1.10	1.00	1.02	0.02	2.21
2	2.08	2.10	2.12	2.05	2.09	0.09	4.39
3	3.14	3.21	3.28	3.13	3.19	0.19	6.30
4	4.26	4.09	4.41	4.11	4.22	0.22	5.39
5	5.28	5.79	5.56	5.19	5.46	0.46	9.12
6	6.34	6.81	6.51	6.45	6.53	0.53	8.80
7	7.30	7.80	7.53	7.34	7.49	0.49	7.03
8	8.34	8.92	8.78	8.67	8.68	0.68	8.46
9	9.51	10.15	9.68	9.48	9.70	0.70	7.83
10	10.57	10.94	10.75	10.17	10.61	0.61	6.08
Grand means						0.40	6.56

the antemortem photograph is known, and the subject is looking directly at the camera.

Calibration of palpebral fissure length using the hat insignia dimensions provided improved and more consistent estimates of SCD: error decreased from a mean of 6.6% (Table 5) to -1.6% (Table 6). Clearly, then inanimate objects of known size, if included in the photograph and falling close to the focal plane and in an orientation that does not compromise their measurement, should be used to provide enhanced estimates. While inanimate objects have previously been used for scaling facial photographs to life size, the difference here is that the measurements are used to calibrate the anatomical measurement of the palpebral fissure length making them closer to the individual values and thereby enhancing the SCD estimation. The inanimate object length is not used for any scaling of the image to life size.

PerspectiveX estimates of SCD were equally good for subadults as they were for adults (Table 5) using the mean palpebral fissure length data provided by Farkas (49).

Repeatability of *PerspectiveX* and SCD Estimation for Rotated Faces

Under different lighting conditions using three new subjects (plus one of the original subjects from Study 1), *PerspectiveX* performed equally well for nonrotated faces that were directly looking into the camera, as it did in Study 1 (Tables 7 and 8), yielding comparable mean SCD errors of 6.1%; range = 4.9–8.8%). Moreover, accuracies held below 10% for the 10° face rotations. As expected errors increased for 20° and 30° rotations, but not so substantially as to make the predictions useless: grand means = 13.5 and 14.4%, respectively. At these error rates, estimated SCDs can be used as accurate predictors for any SCDs >2 m (Table 5). Errors at any given ground truth distance were relatively constant at a mean value of 11%. Attempts to correct for rotation following general protocols of Sekharan (21) provided no evidence of improvement (in fact, they were much worse). These attempts at correction were further hampered by the disappearance of the far exocanthion behind the eyeball, or the far endocanthion behind the bridge of the nose, preventing analysis at face rotations $\geq 20^\circ$. Consequently, these attempts at improving estimates by correcting for head rotation will not be further discussed.

TABLE 6—Mean SCD estimation using *PerspectiveX* and a within image object of known size to calibrate palpebral fissure length in Study 1 for two adults and two subadults.

Ground Truth SCD (m)	<i>PerspectiveX</i> Estimated SCD (m) Using Within Photograph Calibration Object (UQ insignia)					Mean Error (m)	Mean Error (%)
	Subjects				Mean		
	1	2	3	4	Mean		
1	0.89	0.87	0.99	0.91	0.91	−0.09	−8.59
2	1.91	1.85	1.97	1.93	1.92	−0.08	−4.20
3	2.92	2.92	3.01	2.91	2.94	−0.06	−1.92
4	3.89	3.92	4.02	3.78	3.90	−0.10	−2.46
5	4.93	4.99	5.04	4.85	4.95	−0.05	−0.94
6	5.88	5.90	6.02	5.74	5.88	−0.12	−1.93
7	6.88	6.88	7.01	7.59	7.09	0.09	1.24
8	7.84	7.93	8.08	8.75	8.15	0.15	1.89
9	8.86	8.89	8.98	9.88	9.15	0.15	1.69
10	9.86	9.88	10.10	9.90	9.93	−0.07	−0.66
Grand means						−0.02	−1.59

SCD Estimation Using Digital Metadata and Comparisons to *PerspectiveX*

The metadata proved to be highly unreliable for precise SCD estimates, to the point of being almost entirely useless. Most point-and-shoot cameras that were trialed did not include a SCD measurement in the metadata and while both of the full-frame digital SLRs did, they were not reported in identical format. That is, the 6D Canon reported two distances: a *Focus Distance Lower* and a *Focus Distance Upper*, while the Nikon reported a single *Focus Distance*; but none of these three statistics provided good approximations of the ground truth SCD with mean absolute error across the 10 m range being on average: 14%, 127%, and 62%, respectively. The one point-and-shoot camera that did report a *Focus Distance* (Olympus Stylus 790SW) gave an astonishing average error of 675%. These values are generally much too large to offer any value to craniofacial superimposition.

Canon's 6D *Focus Distance Lower* provided the most accurate metadata for SCD, and was generally below 10% error up to a SCD of 7 m, but broke down at larger SCD: 20%, 30% and 104% error at 8 m, 9 m, and 10 m, respectively. The Canon 6D *Focus Distance Lower* only beat *PerspectiveX* at the 1 and 2 m distances where the *PerspectiveX* percentage error was halved:

TABLE 7—Absolute mean errors (m) for SCD estimation using *PerspectiveX* with rotated head positions in Study 2.

Ground Truth SCD (m)	Degree of Head Rotation				
	Anterior View (0 degrees)	10 degrees	20 degrees	30 degrees	Mean
1	0.09	0.08	0.13	0.16	0.11
2	0.12	0.15	0.31	0.26	0.21
3	0.15	0.21	0.44	0.43	0.31
4	0.22	0.30	0.50	0.52	0.38
5	0.31	0.35	0.67	0.63	0.49
6	0.30	0.59	0.77	0.93	0.65
7	0.39	0.61	0.95	1.06	0.75
8	0.44	0.59	1.14	0.99	0.79
9	0.61	1.16	1.19	1.39	1.09
10	0.64	0.68	1.21	1.68	1.05
Mean	0.33	0.47	0.73	0.80	

TABLE 8—Absolute mean errors (%) for SCD estimation using *PerspectiveX* with rotated head positions in Study 2.

Ground Truth SCD (m)	Degree of Head Rotation				Mean
	Anterior View (0 degrees)	10 degrees	20 degrees	30 degrees	
1	8.8	8.4	12.8	15.9	11.5
2	5.9	7.7	15.4	13.1	10.5
3	4.9	6.9	14.8	14.2	10.2
4	5.6	7.5	12.5	12.9	9.6
5	6.1	7.0	13.4	12.6	9.8
6	5.1	9.9	12.8	15.4	10.8
7	5.6	8.7	13.6	15.2	10.8
8	5.5	7.4	14.2	12.4	9.9
9	6.8	12.9	13.3	15.4	12.1
10	6.4	6.8	12.1	16.8	10.5
Mean	6.1	8.3	13.5	14.4	

Canon 6D = 4% and 3% error, respectively; *PerspectiveX* = 8.8% and 5.9% error, respectively (Table 8). As both of the SCDs translate to the same tolerance band of <1% in PD, there are only marginal improvements of using the Canon 6D metadata above *PerspectiveX* at these extremely short subject-to-camera distances. *PerspectiveX* results were more consistent across the full SCD range, and for this reason, it is the recommended method for craniofacial superimposition over and above the *Focus Distance* metadata from the Canon 6D.

Discussion

Like all skeletal identification protocols, craniofacial superimposition methods must be accurate to limit errors that can otherwise have disastrous consequences, ranging from misidentifications in cases of false-positive results, to serial killers left at large in cases of false-negative outcomes. The convincing tangibility that craniofacial superimposition holds to jurors in the courtroom through dramatic visual demonstrations (2) additionally elevates the requirement for the methods to perform with negligible error and be quantitatively accurate and reliable (18,29). In the past, a major long-standing problem has been the inability to accurately estimate the SCD from the antemortem facial photograph. Far from being impossible to estimate as previously thought (21,23,30), this study shows that the estimation of SCD is a relatively straightforward and simple affair using the face anatomy recorded in anterior view photograph, especially when the head rotation is $\leq 10^\circ$ and antemortem face image is an electronic one. The increasing popularity of digital photography and decline of wet film will increase the utility of this method into the future as electronic media becomes evermore common.

The key to estimating SCD from facial morphology is to use a relatively invariant anatomical trait as the referent (such as palpebral fissure length), thereby making sample means good point estimators for any individual of a particular sex, and age bracket—in the case of adults, a single value for each sex can be used. Other necessary parameters such as focal length of the lens are reliably and easily determined from electronic metadata, but even this does not prevent analysis of traditional wet films where information on focal length could, for example, be obtained from the photographer. A further strength of the *PerspectiveX* algorithm is that it relies on a well-trialed, tested and widely used mathematical formula (see e.g., (37)).

In this study, *PerspectiveX* was found to perform as well for children (7 and 9 years of age) as it did for adults. Accuracies held when different participants or camera operators were used, or photography locations changed. The only minor but by no means fatal problem encountered concerned a requirement to estimate the exocanthion positions on some females whose eyelashes were so dense as to obscure clear view of the exocanthion landmark. This was most strongly manifested at large subject-to-camera distance where resolution of the face was low due to its decreased face size on the image receptor. Even in these cases, however, the estimation of the exocanthion position did not interfere with *PerspectiveX* accuracies (Table 5) partly because exocanthion positions could be sufficiently estimated by extending the eyelid-edge lines, and paying attention to the proximity of neighboring surface anatomy features to triangulate on the probable exocanthion location. Furthermore, at larger distances the tolerance window for SCD error (and palpebral fissure length measurements) was much larger reducing the requirement for highly accurate measurements.

Somewhat surprisingly, the raw palpebral fissure lengths measured from the rotated faces worked for SCD estimation. Consequently, at >2 m, *PerspectiveX* can still be used for SCD estimates, so long as head rotation does not exceed 30° . Although not specifically tested here, larger head rotations will likely produce very large inaccuracies for the *PerspectiveX* algorithm. This does not detract from the methods' utility for almost any facial photograph where head rotation is orientated toward the camera, and it does not preclude use of the *PerspectiveX* algorithm in profile view if a different, but sufficiently invariant anatomical trait could be identified to replace the palpebral fissure length and serve as the photographic referent of known object size.

For all subjects, across the 10 m distances investigated, SCD estimation by the *PerspectiveX* algorithm was found to be superior to camera metadata reports of SCD. Consequently, using the metadata reports of SCD as recommended elsewhere in the mainstream literature (28) is not advisable, unless specific tests of the metadata records have been conducted to validate the estimates—as, for example, undertaken herein for the Canon 6D when SCDs are <2 m. This further raises red flags for the acceptance of other recently advocated practices labelled “best practices” (28) without qualification or validation testing.

To facilitate the calculation of SCD in forensic casework, a *PerspectiveX* calculator has been added to CRANIOFACIALidentification.com. This R GUI enables practitioners to input the required four parameters (f , A , x , and y) of Equation (1) to calculate SCD from facial photographs at the click of a button. An SCD point estimate result is returned along with the 99% confidence limits using the extremes of the palpebral fissure length values specified in the data entry, or according to Farkas et al. (49,51,52) when using the provided default settings.

Acknowledgments

Thanks go to Sgt Darren Bails (South Australian Police) for useful discussions about *Exif* metadata, comments on an earlier version of this paper, and directions to *Jeffrey's Online Exif Viewer*. Thanks go to Jodi Caple and Andrea Murphy for operating the camera while the author served as a subject in this study, and to several participants who agreed to publication of their facial photographs.

References

- Taylor JA, Brown KA. Superimposition techniques. In: Clement JG, Ranson DL, editors. *Craniofacial identification in forensic medicine*. London, U.K.: Hodder Arnold, 1998;151–64.
- Ubelaker DH. Craniofacial superimposition: historical review and current issues. *J Forensic Sci* 2015;60(6):1412–9.
- Stephan CN. Craniofacial identification: techniques of facial approximation and craniofacial superimposition. In: Blau S, Ubelaker DH, editors. *Handbook of forensic anthropology and archaeology*. Walnut Creek, CA: Left Coast Press, 2009;304–21.
- Yoshino M. Craniofacial superimposition. In: Wilkinson CM, Rynn C, editors. *Craniofacial identification*. Cambridge, U.K.: Cambridge University Press, 2012;238–53.
- Austin D. Video superimposition at the C.A. Pound laboratory 1987 to 1992. *J Forensic Sci* 1999;44(4):695–9.
- Helmer R, Schimmler J, Rieger J. Zum Beweiswert der Schadelidentifizierung mit Hilfe der Video-Bildmischtechnik unter Berücksichtigung der kranio-metrischen Individualität menschlicher Schadel. *Zeitschrift für Rechtsmedizin* 1989;102(7):451–9.
- Rosenblatt A. Digging for the disappeared: forensic science after atrocity. Stanford, CA: Stanford University Press, 2015.
- Helmer RP, Schimmler JB, Rieger J. On the conclusiveness of skull identification via the video superimposition technique. *Canadian J Forensic Sci* 1989;22(2):177–94.
- Jayaprakash PT. Conceptual transitions in methods of skull-photo superimposition that impact the reliability of identification: a review. *Forensic Sci Int* 2015;246:110–21.
- Sekharan PC. The problems of positioning skulls for video superimposition technique. *Canadian J Forensic Sci* 1989;22(1):21–5.
- Pearson K, Morant GM. The Wilkinson head of Oliver Cromwell and its relationship to busts, masks and painted portraits. *Biometrika* 1934;26:18–378.
- Glaister J, Brash JC. *Medico-legal aspects of the Ruxton case*. Baltimore, MD: William Wood and Co., 1937.
- Fenton TW, Heard AN, Sauer NJ. Skull-photo superimposition and border deaths: identification through exclusion and the failure to exclude. *J Forensic Sci* 2008;53(1):34–40.
- Yoshino M, Imaizumi K, Miyasaka S, Seta S. Evaluation of anatomical consistency in craniofacial superimposition images. *Forensic Sci Int* 1995;74:125–34.
- Chai D-S, Lan Y-W, Tao C, Gui R-J, Mu Y-C, Feng J-H, et al. A study on the standard for forensic anthropological identification of skull-image superimposition. *J Forensic Sci* 1989;34(6):1343–56.
- Jayaprakash PT, Singh B, Hassan NFN, Yusop RAAM. Computer aided video superimposition device: a novel contribution to skull based identification in Malaysia. *HLth Environ J* 2010;1(1):65–74.
- Koelmeyer TD. Videocamera superimposition and facial reconstruction as an aid to identification. *Am J Forensic Med Path* 1982;3(1):45–8.
- Gordon GM, Steyn M. An investigation into the accuracy and reliability of skull-photo superimposition in a South African sample. *Forensic Sci Int* 2012;3:198.e1–e6.
- Brown KA. Developments in cranio-facial superimposition for identification. *J Forensic Odonto-Somatol* 1983;1(2):57–64.
- Brown KA. The Truro murders in retrospect: a historical review of the identification of the victims. *Ann Acad Med Sing* 1993;22(1):103–6.
- Sekharan PC. Positioning the skull for superimposition. In: İşcan MY, Helmer RP, editors. *Forensic analysis of the skull*. New York, NY: Wiley-Liss, 1993;105–18.
- Sekharan PC. A revised superimposition technique for identification of the individual from the skull and photograph. *J Crim Law Criminol Pol Sci* 1971;62(1):107–13.
- Sekharan PC. A scientific method for positioning of the skull for photography in superimposition studies. *J Pol Sci Admin* 1973;1(2):232–40.
- Sauer NJ, Michael AR, Fenton TW. Human identification using skull-photo superimposition and forensic image comparison. In: Dirkmaat D, editor. *A companion to forensic anthropology*. West Sussex, U.K.: Wiley-Blackwell, 2012;435.
- Helmer RP. Identification of the cadaver remains of Josef Mengele. *J Forensic Sci* 1987;32(6):1622–44.
- Marshall D. *Killing for pleasure*. Sydney, Australia: Random House, 2006.
- Pudney J. *The bodies in the Barrels murders*. London, U.K.: John Blake Publishing Ltd, 2006.
- Damas S, Wilkinson C, Kahana T, Veselovskaya E, Abramov A, Jankauskas R, et al. Study on the performance of different craniofacial superimposition approaches (II): best practices proposal. *Forensic Sci Int* 2015;257:504–8.
- Austin-Smith D, Maples WR. The reliability of skull/photograph superimposition in individual identification. *J Forensic Sci* 1994;39(2):446–55.
- Lan Y, Cai D. Technical advances in skull-to-photo superimposition. In: İşcan MY, Helmer RP, editors. *Forensic analysis of the skull*. New York, NY: Wiley-Liss, 1993;119–29.
- Gordon GM, Steyn M. A discussion of current issues and concepts in the practice of skull-photo/craniofacial superimposition. *Forensic Sci Int* 2016;262(287):e1–4.
- Dorion RBJ. Photographic superimposition. *J Forensic Sci* 1983;28(3):724–34.
- Jayaprakash PT, Hashim N, Yusop RAAM. Relevance of Whitnall's tubercle and auditory meatus in diagnosing exclusions during skull-photo superimposition. *Forensic Sci Int* 2015;253:131.e1–e10.
- İşcan MY, Steyn M. *The human skeleton in forensic medicine*, 3rd edn. Springfield, IL: Charles C Thomas, 2013.
- Maat GJR. The positioning and magnification of faces and skulls for photographic superimposition. *Forensic Sci Int* 1989;41:225–35.
- Gavan JA, Washburn SL, Lewis PH. *Photography: an anthropometric tool*. *Am J Phys Anthropol* 1952;10:331–53.
- Kingslake R. *Optics in photography*. Washington, DC: SPIE, 1992.
- Scully B, Nambiar P. Determining the validity of Furue's method of craniofacial superimposition for identification. *Ann Dent Univ Mal* 2002;9:17–22.
- Taylor J. Distortion in craniofacial video superimposition [Masters thesis]. Adelaide, Australia: The University of Adelaide, 1991.
- Titlbach Z. Beiträge zur Bewertung der Superprojektionsmethode zur Identifizierung unbekannter Skelettfunde. *Kriminalistik und forensische Wissenschaften*. Berlin, Germany: German Publisher of Sciences, 1970;179–90.
- Stephan C. Facial approximation and craniofacial superimposition. In: Smith C, editor. *Encyclopedia of global archaeology*. New York, NY: Springer Science+Business Media, 2014;2721–9.
- Grüner O, Reinhard R. Eine photographische verfahren zur schädelidentifizierung. *Deutsche Zeitschrift für Gerichtliche Medizin* 1959;47:247–56.
- Miyasaka S, Yoshino M, Imaizumi K, Seta S. The computer-aided facial reconstruction system. *Forensic Sci Int* 1995;74:155–65.
- Elišová H, Krsek P. Superimposition and projective transformation of 3D object. *Forensic Sci Int* 2007;167:146–53.
- Hashimoto M. A study of the superimposition technique as a positive identification method. *Shikawa Gakuho* 1992;92:409–34.
- Stephan C. Perspective distortion in craniofacial superimposition: logarithmic decay curves mapped mathematically and by practical experiment. *Forensic Sci Int* 2015;257:e1–8.
- Farkas LG. *Anthropometry of the head and face*. New York, NY: Raven, 1994.
- Bookstein FL. *Morphometric tools for landmark data: geometry and biology*. Cambridge, U.K.: Cambridge University Press, 1991.
- Farkas LG, Hreczko TM, Katic M. Craniofacial norms in North American Caucasians from birth (one year) to young adulthood. In: Farkas LG, editor. *Anthropometry of the head and face*. New York, NY: Raven Press, 1994;241–336.
- Caroline PJ, André MP. The effect of corneal diameter on soft lens fitting, part 1. *Contact Lens Spect* 2002;17(4):56.
- Farkas LG, Ngim RCK, Lee ST. Craniofacial norms in 6-, 12-, and 18-year-old Chinese subjects. In: Farkas LG, editor. *Anthropometry of the head and face*. New York, NY: Raven Press, 1994;337–46.
- Farkas LG, Venkatadri G, Gubbi AV. Craniofacial norms in young adult African-Americans. In: Farkas LG, editor. *Anthropometry of the head and face*. New York, NY: Raven Press, 1994;347–52.

Additional information and reprint requests:

Carl N. Stephan, Ph.D.

Laboratory for Human Craniofacial and Skeletal Identification

School of Biomedical Sciences

The University of Queensland

Brisbane 4072

Australia

E-mail: c.stephan@uq.edu.au